

ANALYSIS OF ANTARCTIC ICEBERG AND SEA ICE MELTING PATTERNS USING QUIKSCAT

Keith M. Stuart and David G. Long

Brigham Young University
Microwave Earth Remote Sensing Laboratory
459 CB, Provo, UT 84602

ABSTRACT

QuikSCAT tracking of Antarctic icebergs is discussed, and iceberg movement trends are illustrated. Iceberg melting factors are explored and a backscatter time-series is presented. Interactions between iceberg and sea ice are examined using QuikSCAT data. To improve QuikSCAT sea ice mapping capability, a threshold algorithm to detect polynyas is developed. The 2006-2007 Antarctic ablation season is analyzed and correlations between polynya formation and sea ice melting are explored. General sea ice melting patterns are discussed, and statistics are derived from QuikSCAT's life mission and compared with SSM/I measurements. This study finds that while average Antarctic sea ice coverage is increasing, minimum sea ice extent is decreasing.

1. INTRODUCTION

Knowledge of Antarctic iceberg and sea ice melting patterns are valuable tools in understanding many geophysical and biological processes. Coupled with global oceanic and atmospheric cycles, ice melting patterns are considered a sensitive indicator of global climate change. As a result, an in-depth study of iceberg and sea ice melting patterns is necessary to better understand climate conditions and general trends of our planet.

To aid in gathering this information, satellite sensors such as SSM/I and SeaWinds are used [1]. While SSM/I is effective at sea ice detection and classification, it is often difficult to detect all but the largest icebergs due to low resolution compared with iceberg size and a low contrast between icebergs and sea ice.

This paper discusses the utility of using the SeaWinds scatterometer aboard QuikSCAT to detect and analyze the melting trends of both Antarctic icebergs as well as Antarctic sea ice. The ability of QuikSCAT to detect and track icebergs and sea ice is correlated with the National Ice Center (NIC) iceberg database and SSM/I data sea ice maps [2]. In addition, image reconstruction techniques are employed which increases QuikSCAT's effective resolution.

2. ICEBERG TRACKING

QuikSCAT's backscatter values are a function of composition and surface roughness which differ greatly between glacial ice, first-year sea ice and open water. Icebergs exhibit a characteristic high backscatter at both vertical and horizontal polarizations in QuikSCAT's radar backscatter datasets. Oceanic returns are dependent on polarization and wind conditions with h-pol having the smallest return. Therefore, in an effort to maximize backscatter

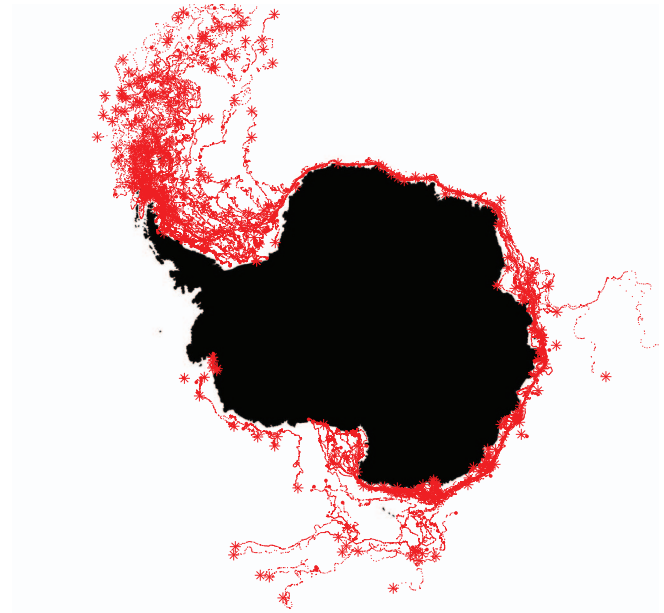


Fig. 1. A depiction of Antarctic icebergs detected by QuikSCAT from 1999-2007. The “.” and “*” markers represent initial and final tracking positions respectively. Note the path that many icebergs travel counter-clockwise around the perimeter of Antarctica until they accumulate in the Weddell Sea. This plot illustrates the region where icebergs travel from the Weddell Sea to the Scotia Sea, sometimes called “iceberg alley.”

contrast between glacial ice and open water, horizontal polarization is normally used in iceberg detection.

Because tabular icebergs frequently exist beyond a single ablation season, they experience several localized environmental conditions which affect their physical properties and thus their backscatter returns. As a result, a general melting analysis is presented using a backscatter time-series. However, since coastal conditions vary depending on location, scale analysis is aided with an understanding of general iceberg movement.

Due to the ratio of iceberg mass under the ocean's surface, oceanic currents frequently dominant large iceberg movements. Near the coast of Antarctica, these currents sweep icebergs counter-clockwise until they accumulate in the Weddell Sea, see Fig. 1. They are then propelled into the Scotia Sea and around 60°S are swept



Fig. 2. Number of Antarctic icebergs detected by QuikSCAT (solid) and reported by the NIC (dashed) from 1999-2007. QuikSCAT reports all Antarctic iceberg positions daily; however, because the NIC reports positions periodically, the NIC iceberg count above is an interpolated estimate (i.e. if the NIC reports the same iceberg on JD10 & JD50, this graph counts the iceberg for JD10-50).

into the Antarctic Circumpolar Current (ACC). By the time most icebergs reach the ACC, the icebergs have broken up, backscatter intensity blends into ocean noise and the remaining fragments are no longer detectable by Seawinds. However, some large icebergs have been tracked as far north as 48°S .

Validation of iceberg positions is accomplished by correlating information with the NIC. Brigham Young University's Microwave Earth Remote Sensing (MERS) Laboratory Antarctic iceberg database contains nearly all NIC icebergs on record in addition to over 200 untracked icebergs since 1999. Historical and real-time locations are provided to the NIC and other users at [3].

During the Antarctic winter, icebergs are easily detected in QuikSCAT backscatter images due to their significant volume scattering. This signature remains consistent until the Antarctic ablation season when surface temperature variations commonly cross the glacial ice's melting threshold. The resulting state changes result in significant backscatter variations which decrease QuikSCAT's ability to detect icebergs in the austral summer. Figure 2 presents the number of icebergs detected by QuikSCAT and reported by the NIC from 1999-2007. The fluctuations in the annual QuikSCAT iceberg count are artifacts of the ablation season backscatter fluctuations. Also note the higher iceberg count in 2002 which correlates with the breakup of the Larsen-B ice shelf.

While each iceberg has a unique backscatter fluctuation as a function of size, location and local weather conditions, periodic trends are recognizable in an average time-series. Figure 3 illustrates the average iceberg backscatter from 1999-2007 by quadrant. Corresponding iceberg counts are provided in order to gain an understanding into the amount of averaging performed. Note that where the iceberg count is sufficiently high, a seasonally periodic backscatter signature is observable. Also note the annual iceberg count trends due to seasonal backscatter fluctuations that result from melting surface glacial ice during the ablation season. From Fig. 3, trends in the number of icebergs calved in each quadrant as well as a description of general iceberg flow around Antarctica is also observable.

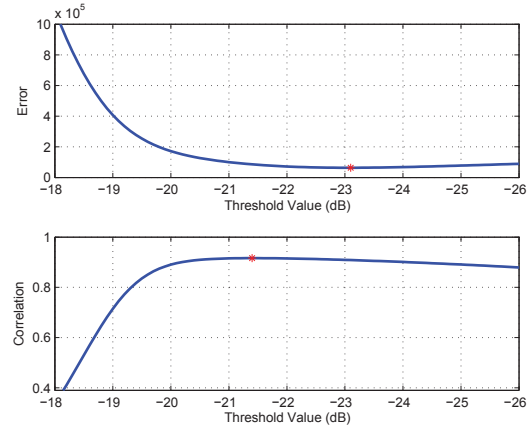


Fig. 4. Average RMS Error and correlation of the difference in polynya surface area detected by the QuikSCAT and SSM/I satellites vs. h-pol backscatter detected by QuikSCAT from 1999-2007. The "*" markers highlight extrema.

3. ICEBERG AND SEA ICE INTERACTIONS

An important factor in analyzing iceberg movement is an understanding of the coupled effects of icebergs with sea ice. While the deep draft of large tabular icebergs results in their being entrained in deep water currents, their movement and evolution are affected by nearby sea ice since sea ice protects the iceberg from wave action. In addition, this relationship affects localized sea ice formation and melting cycles.

For example, as seen in Fig. 1, most icebergs follow a counter-clockwise path from their calving point around Antarctica until ejected into the Scotia Sea. Icebergs that deviate from this path, such as the icebergs with paths to the right and to the bottom of Fig. 1, are frequently carried with sea ice flowing away from the glacial continent during the Antarctic winter which melts back during the Austral summer. Another interaction of icebergs and sea ice is the ability of icebergs to surround areas of sea ice and impede recession and in extreme cases prevent sea ice melting altogether during the Antarctic summer.

4. SEA ICE & POLYNIA DETECTION

Studies have established that SeaWinds can map sea ice using a dual-polarization ratio metric [4]. However, one disadvantage of this algorithm is its rejection of polynyas which have significant surface area and impact nearby sea ice melting.

At Ku-band, polynyas are commonly characterized as areas of low backscatter surrounded by higher backscatter sea ice. As a result, flagging backscatter values less than a given threshold inside the ice mask enables detection of Antarctic polynyas. Our methodology for determining an appropriate threshold involves minimizing the RMS error between the polynya surface area detected by QuikSCAT and an established standard, in this case SSM/I [1, 2]. Figure 4 is a depiction of the RMS difference of polynya area as detected by QuikSCAT and SSM/I versus QuikSCAT backscatter threshold. A threshold of -23.1dB minimizes the RMS error. At this threshold is the correlation of 0.915.

This polynya detection technique relies on the relatively low backscatter signature of ocean water. However, since strong cata-

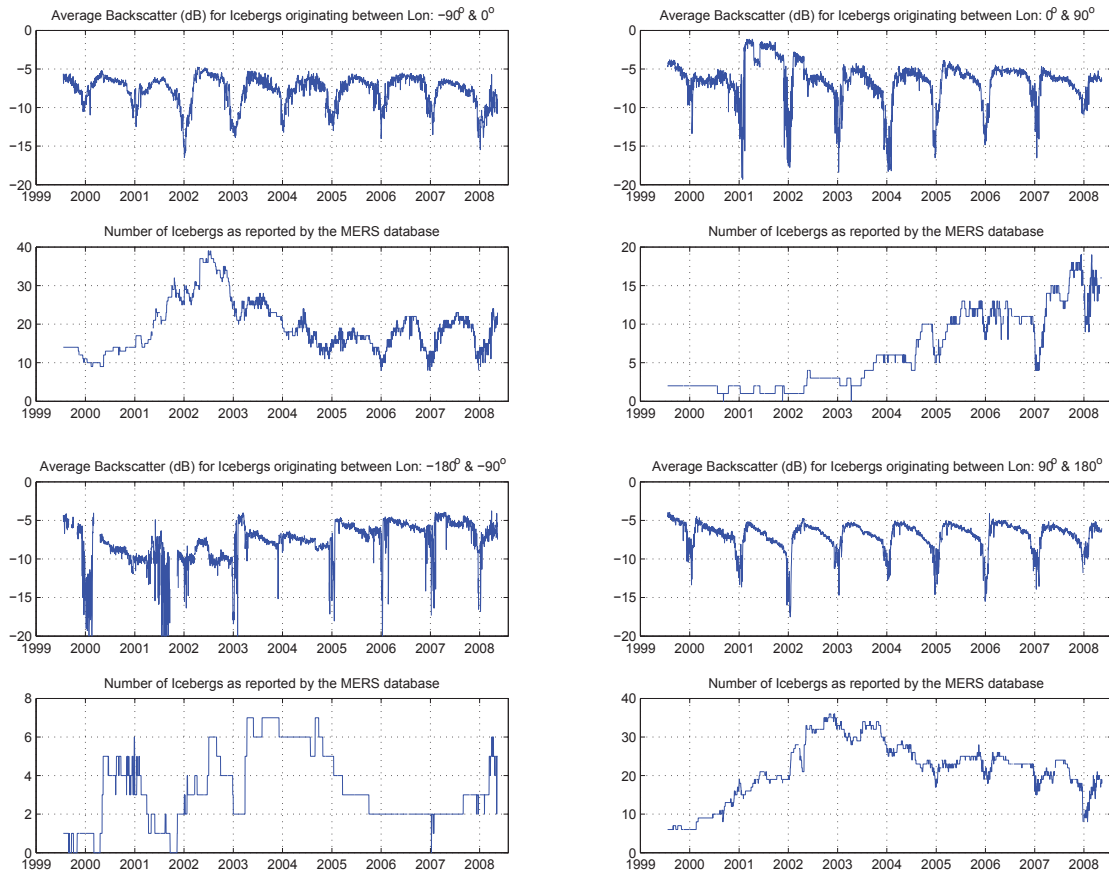


Fig. 3. Average Antarctic iceberg h-pol backscatter detected by QuikSCAT from 1999-2007. Corresponding QuikSCAT iceberg counts are also presented.

batic winds are a common cause of latent-heat polynyas, these same winds frequently roughen the surface of coastal polynyas, increasing backscatter values until they are comparable to that of first-year sea ice. When this occurs, polynya detection accuracy is reduced; nevertheless, this simple algorithm is suitable for large-scale polynya mapping.

5. SEA ICE MELTING PATTERNS

Two general sea ice melting patterns have been observed from QuikSCAT measurements [3]. Figure 5 is an illustration of the 2006-2007 Antarctic ablation season. During the onset of the austral summer, the first trend is the general melting of the north-most sea ice. Figure 5a represents the sea ice at its maximum extent. The melting of the outer-most sea ice is visible on the outer fringes of Fig 5b. The second mark of the austral summer is the formation of several latent-heat polynyas that form around Antarctica’s perimeter. One example is the Ross Sea polynya as seen in Fig. 5b. These polynyas are consistent in location and survive most of the ablation season.

As the warmer equatorial conditions heat ocean currents flowing into the ACC, a smaller number of sensible-heat polynyas form in the main body of Antarctica’s sea ice. These polynyas commonly fluctuate in size and vary in location each year. A notable exception is the polynya which forms at approximately 0°E 65°S every year

as seen in Fig. 5b. This sensible-heat polynya approaches the Ross latent-heat polynya in size until warmer waters melt neighboring sea ice as depicted in Fig. 5c.

As a result of this dual-melting cycle, sea ice is simultaneously melting toward both a lower latitude and towards a higher latitude, resulting in a large ring of sea ice surrounding the glacial continent in the area.

Even though the extent of sea ice coverage varies up to 5% on average between QuikSCAT and SSM/I measurements, both are consistent in overall sea ice trends. Sea ice and polynya cycles from 1999-2007 are illustrated in Fig. 6 with corresponding statistics in Table 1. Note that while sea ice maxima vary up to 3 million square kilometers between years, the observations suggest overall sea ice coverage is increasing while minimum sea ice extent is decreasing.

Table 1. Antarctic sea ice surface area statistics derived from Fig. 6.

Sea Ice Trends	SSM/I		QuikSCAT	
Growing Trend	68100	0.36%	68300	0.38%
Total Trend	49500	0.41%	46700	0.40%
Melting Trend	-97700	-2.15%	-91400	-2.17%

(Units = square kilometers / year)

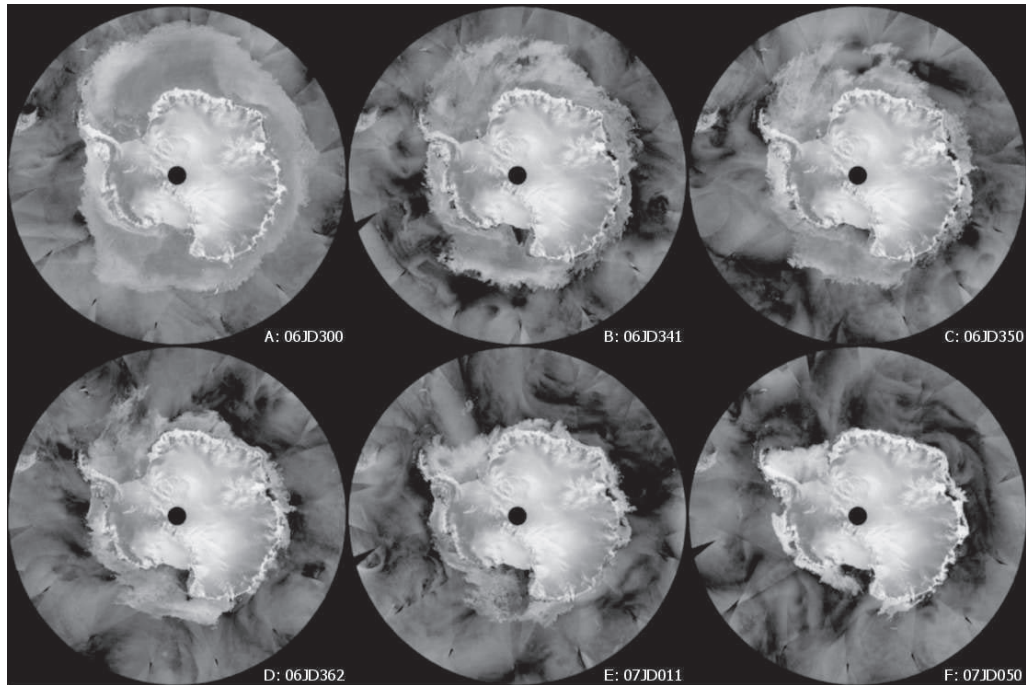


Fig. 5. Southern polar stereographic depiction of QuikSCAT's h-pol backscatter measurements throughout the 2006-2007 Antarctic ablation season. Each image represents Antarctica's glacial continent at center surrounded by varying extents of sea ice. The darkest return is characteristic of open water. a) Sea ice at its maximum (19 million square kilometers); b) Sea ice and initial formations of latent-heat and sensible-heat polynyas; c) Sea ice where the sensible-heat polynya at 0°E & 65°S is exposed and classified as open ocean; d) Continued sea ice reduction; e) Sea ice just before the Ross Sea polynya is dissolved; f) Sea ice at its seasonal minimum (3 million square kilometers).

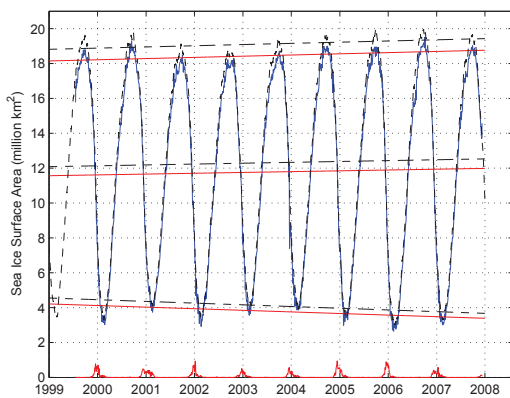


Fig. 6. Antarctic sea ice surface area as detected by both QuikSCAT (solid lines) and SSM/I (dashed lines) from 1999-2007. A least squares fit to the peaks of the annual growing and melting cycles as well as the overall sea ice datasets is also illustrated. The line at the bottom of panel is a plot of the polynya surface area detected by QuikSCAT with the algorithm developed in this paper using a backscatter threshold of -23.1dB

6. CONCLUSION

Macro-scale iceberg and sea ice melting patterns based on QuikSCAT were presented. To better estimate sea ice area, a simple polynya-detection algorithm for QuikSCAT is developed. Sea ice area statistics derived from QuikSCAT measurements show consistency with SSM/I measurements. We conclude that QuikSCAT is an excellent supplementary platform from which to observe iceberg and sea ice melting patterns.

7. REFERENCES

- [1] T. Hunewinkel, T. Markus, and G. C. Heygster, "Improved Determination of the Sea Ice Edge with SSM/I Data for Small-Scale Analyses," *IEEE Transactions on Geoscience and Remote Sensing*, vol. 36, no. 5, 1998.
- [2] National Snow and Ice Data Center, "DMSP SSM/I daily polar-gridded sea ice concentrations, 1999 to 2008," Digital media, update 2008, Edited by K. M. Stuart. Provo, Utah USA: Brigham Young University.
- [3] Microwave Earth Remote Sensing Laboratory, "Scatterometer Climate Record Pathfinder," <http://www.scp.byu.edu/>, update 2008, Edited by K. M. Stuart. Provo, Utah USA: Brigham Young University.
- [4] Q. P. Remund and D. G. Long, "Sea Ice Extent Mapping Using Ku-Band Scatterometer Data," *Journal of Geophysical Research*, vol. 104, no. C5, pp. 11515-11527, 1999.